

Supporting Information

Directional Carrier Transfer in Strongly Coupled Binary Nanocrystal Superlattice Films Formed by Assembly and *in situ* Ligand Exchange at a Liquid-Air Interface

Yaoting Wu[‡], *Siming Li*^{§†}, *Natalie Gogotsi*^{||}, *Tianshuo Zhao*^{||}, *Blaise Fleury*[‡], *Cherie R. Kagan*^{‡||‡}, *Christopher B. Murray*^{‡||*}, and *Jason B. Baxter*^{§*}

[‡]Department of Chemistry, ^{||}Department of Materials Science and Engineering, [‡]Department of Electrical and Systems Engineering, University of Pennsylvania, Philadelphia, Pennsylvania 19104, United States

[§]Department of Chemical and Biological Engineering, Drexel University, Philadelphia, Pennsylvania 19104, United States

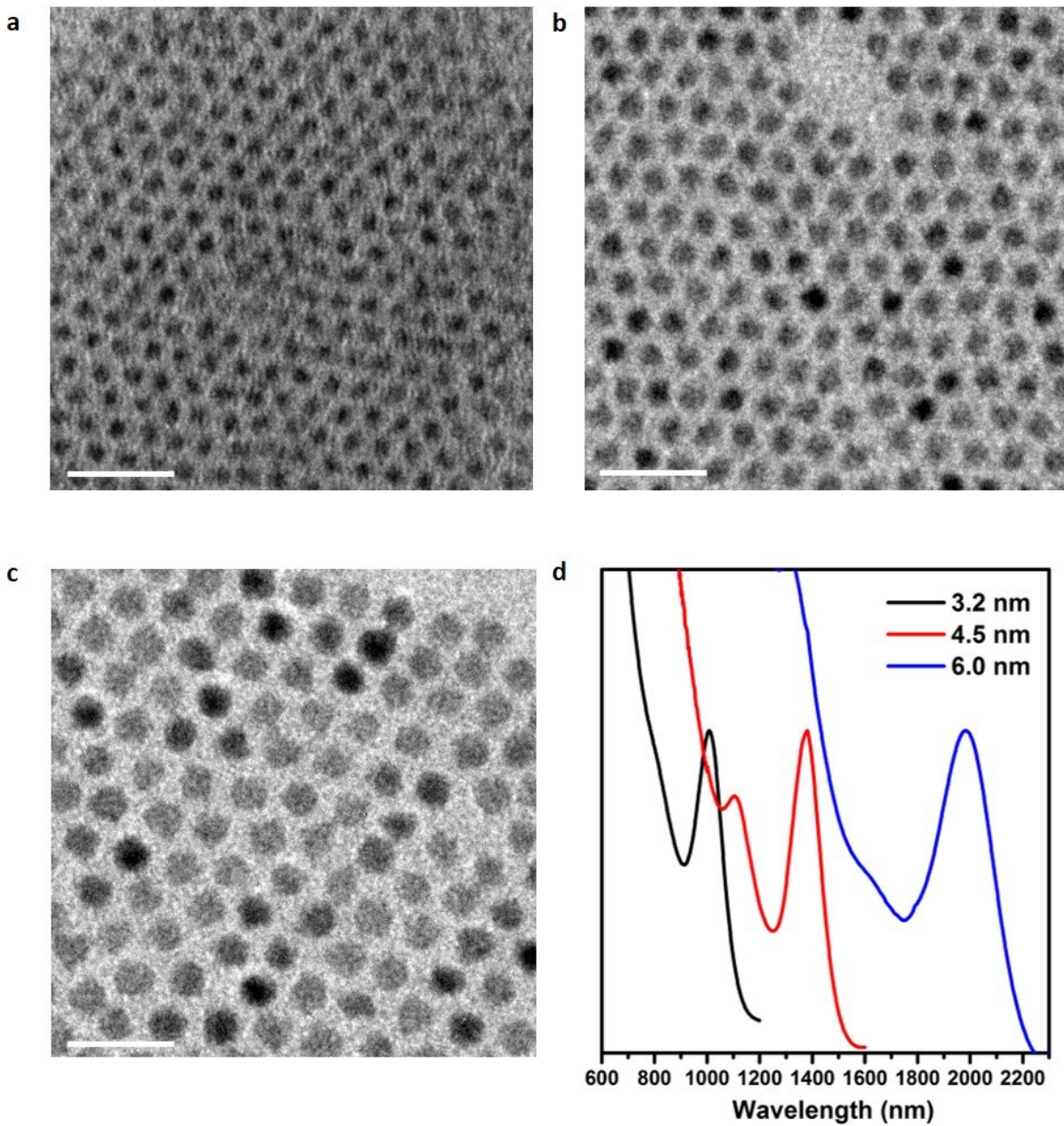


Figure S1. TEM images of PbSe NCs of different size (a) 3.2 ± 0.3 nm, (b) 4.5 ± 0.3 nm and (c) 6.0 ± 0.4 nm. Scale bars represent 20 nm. (d) UV-Vis spectra of corresponding PbSe NCs.

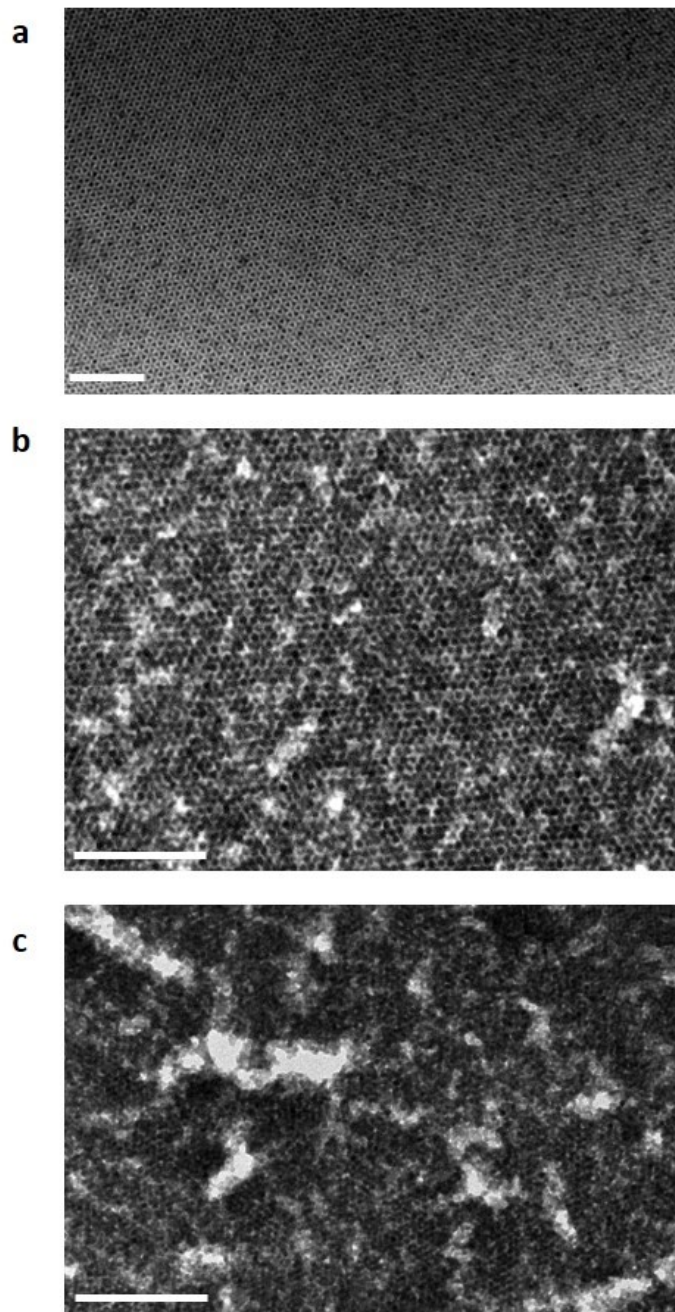
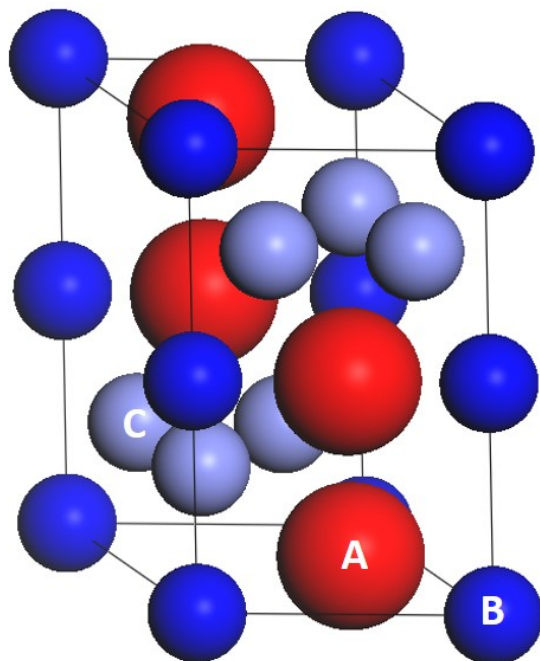


Figure S2. Low magnification TEM images of (a) BNSL film (self-assembled with 4.5 nm and 6.0 nm PbSe NCs), (b) the same BNSL film ligand exchanged on liquid-air interface with MPA, and (c) the same BNSL film ligand exchanged with MPA after the film was transferred to a solid substrate. The scale bar in each image represents 100 nm.



Coordinates of NCs in a MgZn ₂ unit cell			
Labels	x	y	z
A	0.6667	0.6667	0.0620
B	1	1	0
C	0.1695	0.1695	0.2500

Figure S3 and Table S1. Structural models of MgZn₂-type unit cell. A and B are 4.5 nm PbSe NC, and C is 6.0 nm PbSe NC. A, B and C represent three types of PbSe NCs which obtain equivalent coordinates in a unit cell. The 4.5 nm PbSe NCs occupy two different sites, represented by light and dark blue spheres, while the 6.0 nm PbSe NCs are represented by the red spheres. The corresponding coordinates are listed in table S1.

Calculation of the shortest center-to-center inter-particle spacing in MgZn₂-type unit cell.

$$d = \sqrt{(1 - 0.6667)^2 \times a^2 + (1 - 0.6667)^2 \times b^2 + (0 - 0.0620)^2 \times c^2}$$

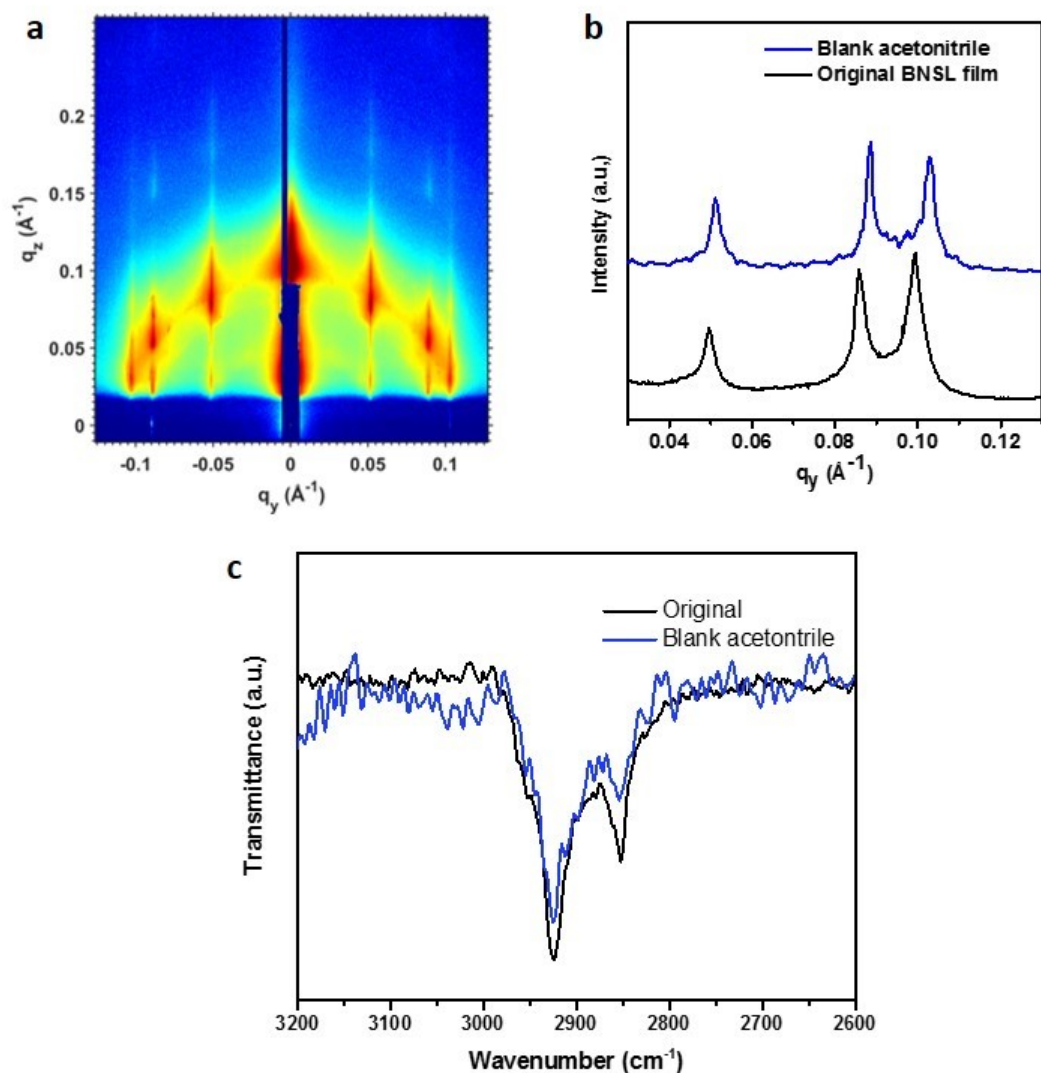


Figure S4. (a) GISAXS pattern of MgZn_2 -type BNSL film (self-assembled with 4.5 nm and 6.0 nm PbSe NC) treated with blank acetonitrile. (b) Linecuts along q_y axis of GISAXS spectra of original film and the one treated with blank acetonitrile. (c) FT-IR spectra of C-H stretching vibrations of the original film and the one treated with blank acetonitrile.

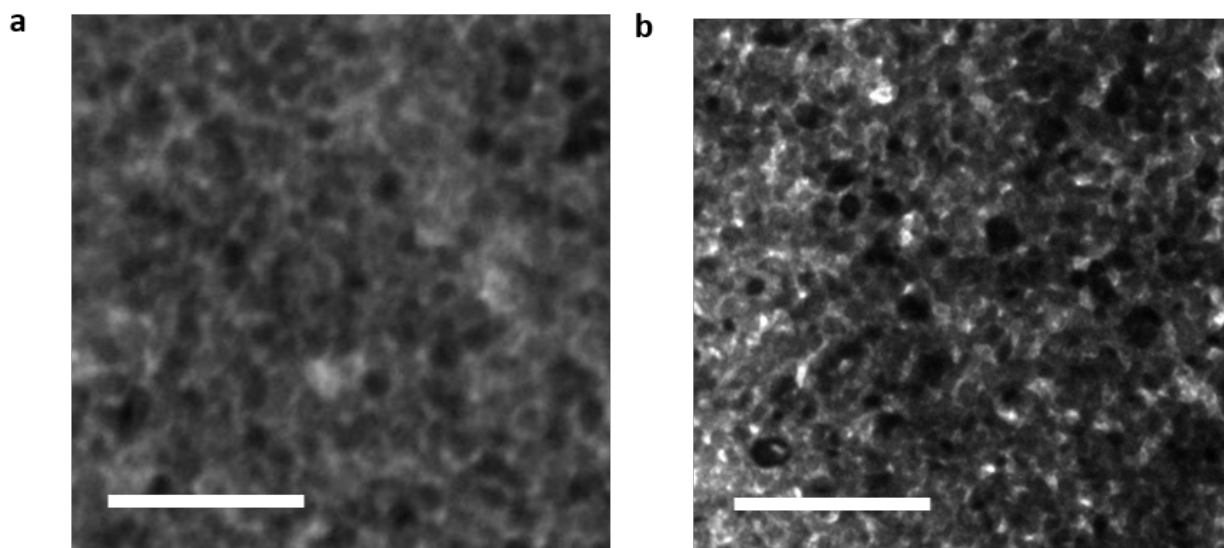


Figure S5. TEM images of BNSL film (self-assembled with 4.5nm and 6.0 nm PbSe NCs) after ligand exchange with (a) 0.1M NH_4SCN in acetonitrile and (b) 0.1 M Formic acid in acetonitrile. Scale bars represent 100 nm.

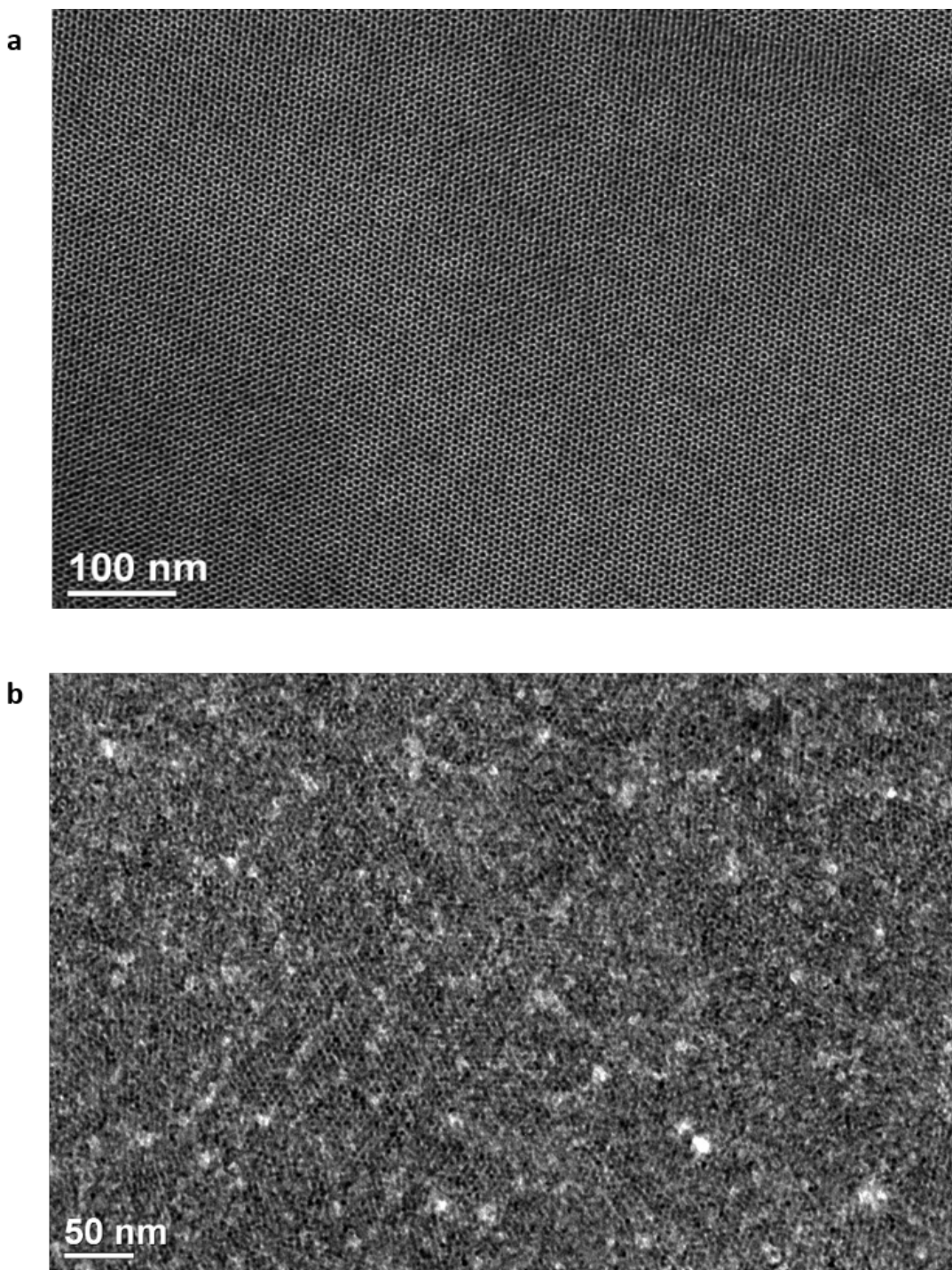


Figure S6. Low magnification TEM images of (a) BNSL film (self-assembled with 3.2 nm and 4.5 nm PbSe NCs) and (b) the same film ligand exchanged with 0.1 M MPA in acetonitrile.

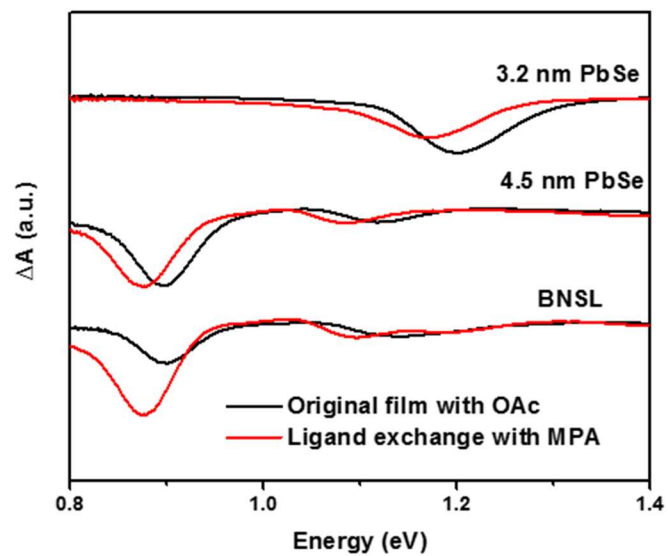


Figure S7. NIR-TA spectra of 3.2 nm NC SL, 4.5 nm NC SL, and corresponding BNSL with original oleic acid ligand (black) and ligand exchange with MPA (red). Spectra selected at pump-probe delay time of 2 ps.

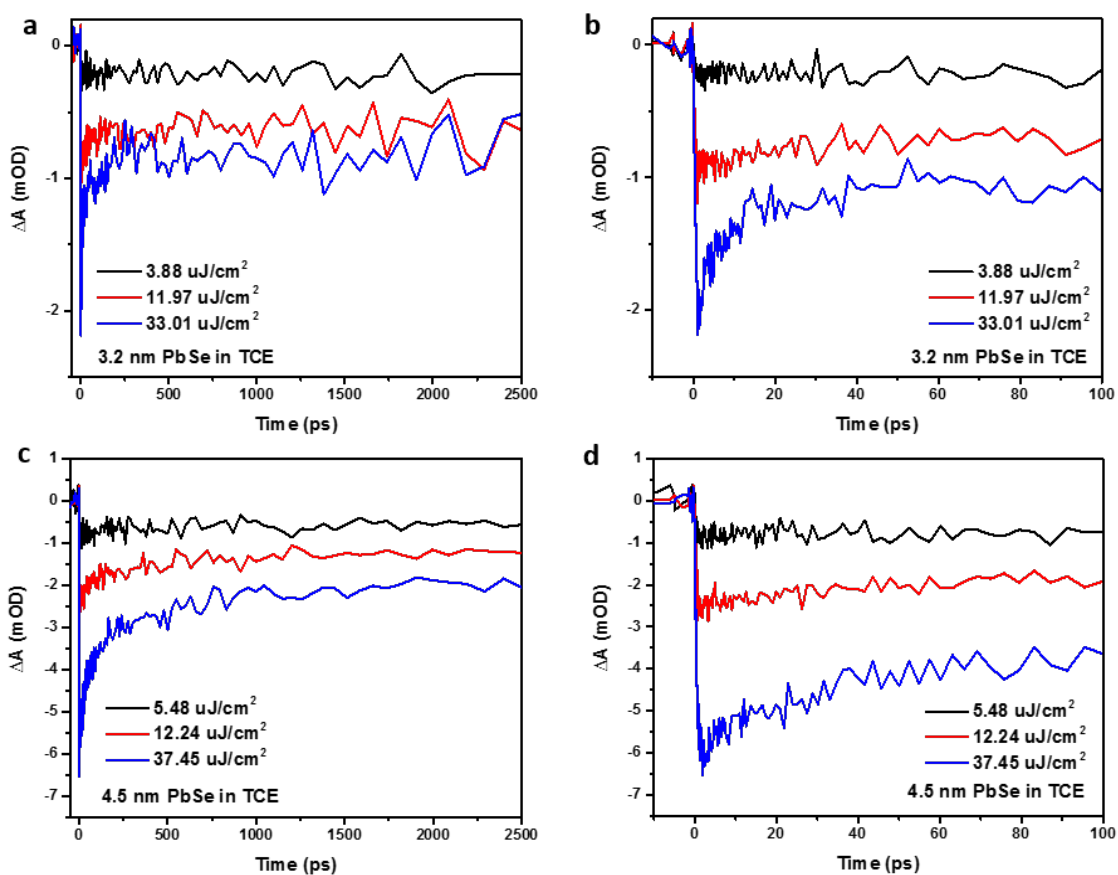


Figure S8. Fluence dependent dynamics of (a, b) 3.2 nm NCs and (c, d) 4.5 nm NCs as colloidal suspension in tetrachloroethylene (TCE). The timescale for a and c is up to 2.5 ns, and b and d is within 100 ps. The lowest fluence trace in both figures shows flat kinetics with negligible amount of Auger recombination.

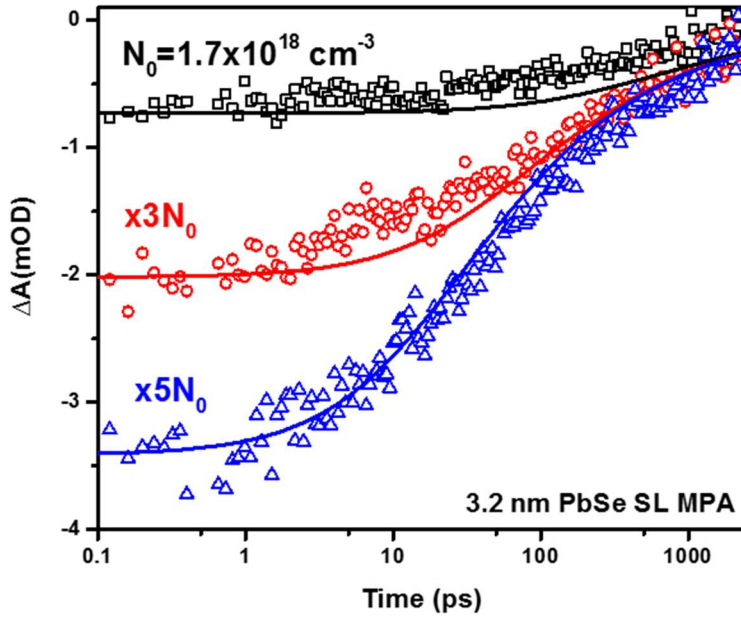


Figure S9. Fluence dependent study of MPA-capped 3.2 nm NC SL film. The solid lines are a global fit with an Auger recombination rate equation. The fluence was $7 \mu\text{J}/\text{cm}^2$ for $N_0 = 1.7 \times 10^{18} \text{ cm}^{-3}$.

Table S2. Fitting parameters and calculated Auger lifetimes at $18 \mu\text{J}/\text{cm}^2$ from dynamic modeling.

	3.2 nm MPA	4.5 nm MPA
k_{Aug}	$5.4 \times 10^{-40} \text{ cm}^6 \text{ ps}^{-1}$	$7.3 \times 10^{-40} \text{ cm}^6 \text{ ps}^{-1}$
N_0	$4.3 \times 10^{18} \text{ cm}^{-3}$	$5.5 \times 10^{18} \text{ cm}^{-3}$
Auger Lifetime	100 ps	45 ps

$$\frac{dn}{dt} = -k_{\text{Aug}} n^3$$

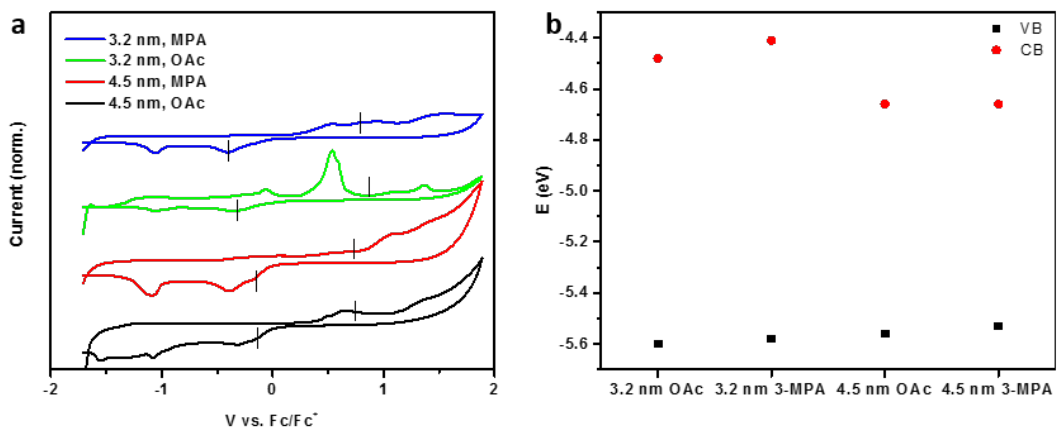


Figure S10. (a) Cyclic voltammetry measurement, and (b) corresponding band edges of 3.2 nm and 4.5 nm PbSe NC thin films with and without MPA ligand exchange.

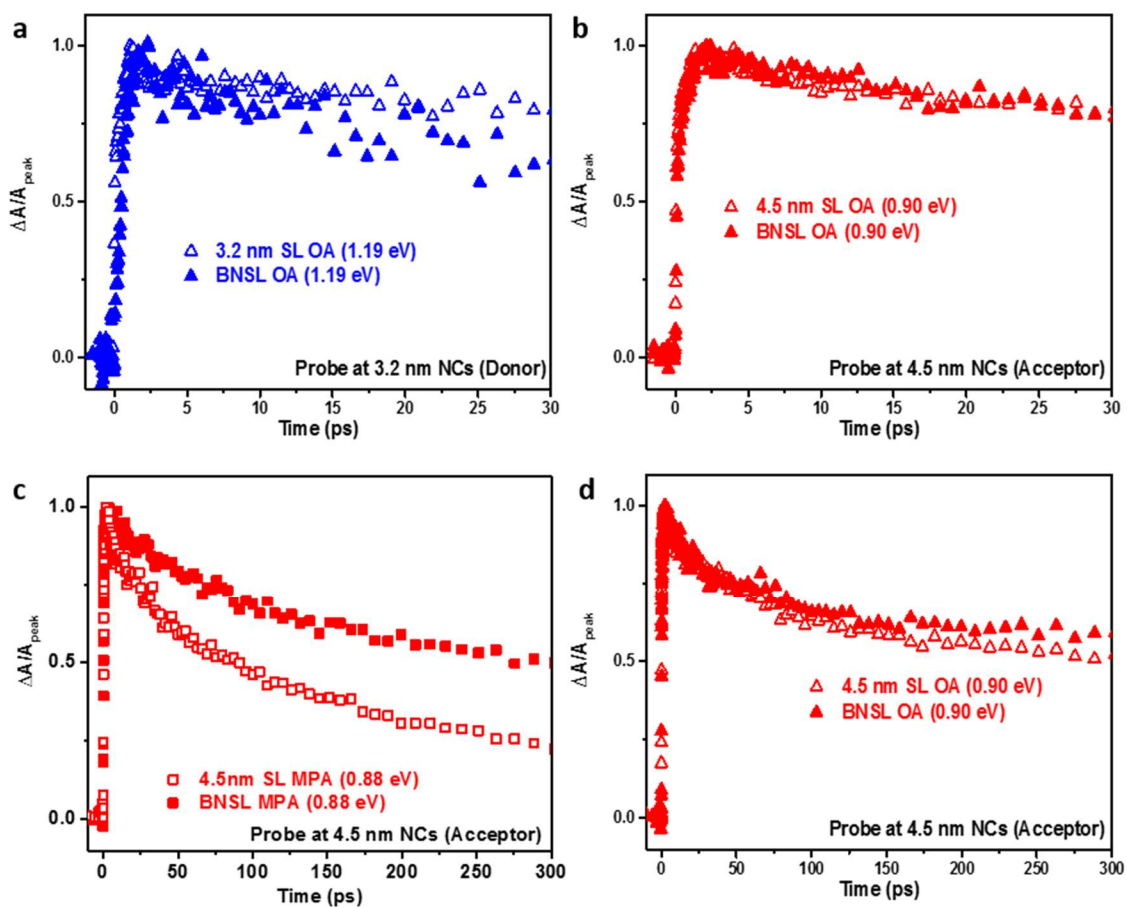


Figure S11. The dynamics of the single-component SL and BNSL of 3.2 nm NCs (a) and 4.5 nm NCs (b) capping with oleic acid within 30 ps. The dynamics of 4.5 nm NCs with (c) and without (d) ligand exchange over 300 ps.

Table S3. Calculation of initial exciton density in NC films. Film thickness was characterized by AFM in Figure S11-12. The lattice constants were simulated from GISAXS patterns of 3.2 nm and 4.5 nm PbSe NC SLs ligand exchanged with MPA. (Figure S13).

Sample (MPA)	Measured Absorbance @ 3.18 eV	Lattice constant (nm)	Film Thickness (nm)	Particle Density (10^{18} cm^{-3})	Calculated Absorbance @ 3.18 eV	Initial Exciton Density (10^{18} cm^{-3})	Average Exciton/NC
3.2 nm SL	0.40	a=b=4.8 c=6.5 (bct)	82	13.4		4.3	0.3
4.5 nm SL	0.41	a=b=6.5 c=9.6 (bct)	65	4.9		5.5	1.1
BNSL	0.41	a=b=9.9 c=17.1	86	7.3	0.42	4.1	0.6
BNSL (3.2 nm)				4.9	0.15	1.5	0.3
BNSL (4.5 nm)				2.4	0.27	2.6	1.1

The particle density of 3.2 nm NCs was calculated based on lattice structure as shown below:

$$C_{3.2nm} = \frac{2}{4.8nm \times 4.8nm \times 6.5nm} = 1.3 \times 10^{19} \text{ cm}^{-3} \text{ as } 2.2 \times 10^{-2} \text{ M}$$

The Beer-Lambert law was used to obtain molar extinction coefficient (ϵ) from the absorbance (A_{abs}), film thickness (l), and particle density (c):

$$A_{abs} = \epsilon l c$$

$$\epsilon_{3.2nm} = \frac{A_{abs_{3.2nm}}}{l_{3.2nm} C_{3.2nm}} = 2.2 \times 10^6 \frac{1}{\text{cm} * \text{M}}$$

We applied the same method to calculate molar extinction coefficient of 4.5 nm PbSe SL :

$$\epsilon_{4.5nm} = 7.7 \times 10^6 \frac{1}{\text{cm} * \text{M}}$$

Since the BNSL contains two species (3.2 nm & 4.5 nm) in known ratios, absorbance of the BNSL could be estimated from properties of each species and the film thickness:

$$A_{abs_{BNSL}} = l_{BNSL} (\epsilon_{3.2nm} C_{BNSL(3.2nm)} + \epsilon_{4.5nm} C_{BNSL(4.5nm)}) = 0.42$$

The calculated absorbance of 0.42 agrees with the value of 0.41 measured by UV-vis.

The fraction of excitons generated in the 4.5 nm NCs in the BNSL was calculated by:

$$\frac{l_{BNSL} \epsilon_{4.5nm} C_{BNSL(4.5nm)}}{A_{abs_{BNSL}}} = \frac{0.27}{0.42} = 0.64$$

Therefore, 64% of the excitons generated with pump photon energy of 3.18 eV originate within the acceptor NCs.

The absorption and film thickness were used to calculate the initial exciton density for a pump fluence of $29.7 \mu\text{J}/\text{cm}^2$:

$$\frac{F(1-10^{-A_{abs}})}{3.18 \text{ eV} \times 1.6 \times 10^{-1} \frac{\text{J}}{\text{eV}} \times l} = \frac{29.7 \mu\text{J}/\text{cm}^2 (1-10^{-0.40})}{3.18 \text{ eV} \times 1.6 \times 10^{-13} \frac{\mu\text{J}}{\text{eV}} \times 82 \text{ nm} \times 10^{-7} \frac{\text{cm}}{\text{nm}}} = 4.3 \times 10^{18} \text{ cm}^{-3} \text{ for } 3.2 \text{ nm SL.}$$

The same equation is applied for 4.5 nm SL and BNSL, and calculated result shown in Table S3.

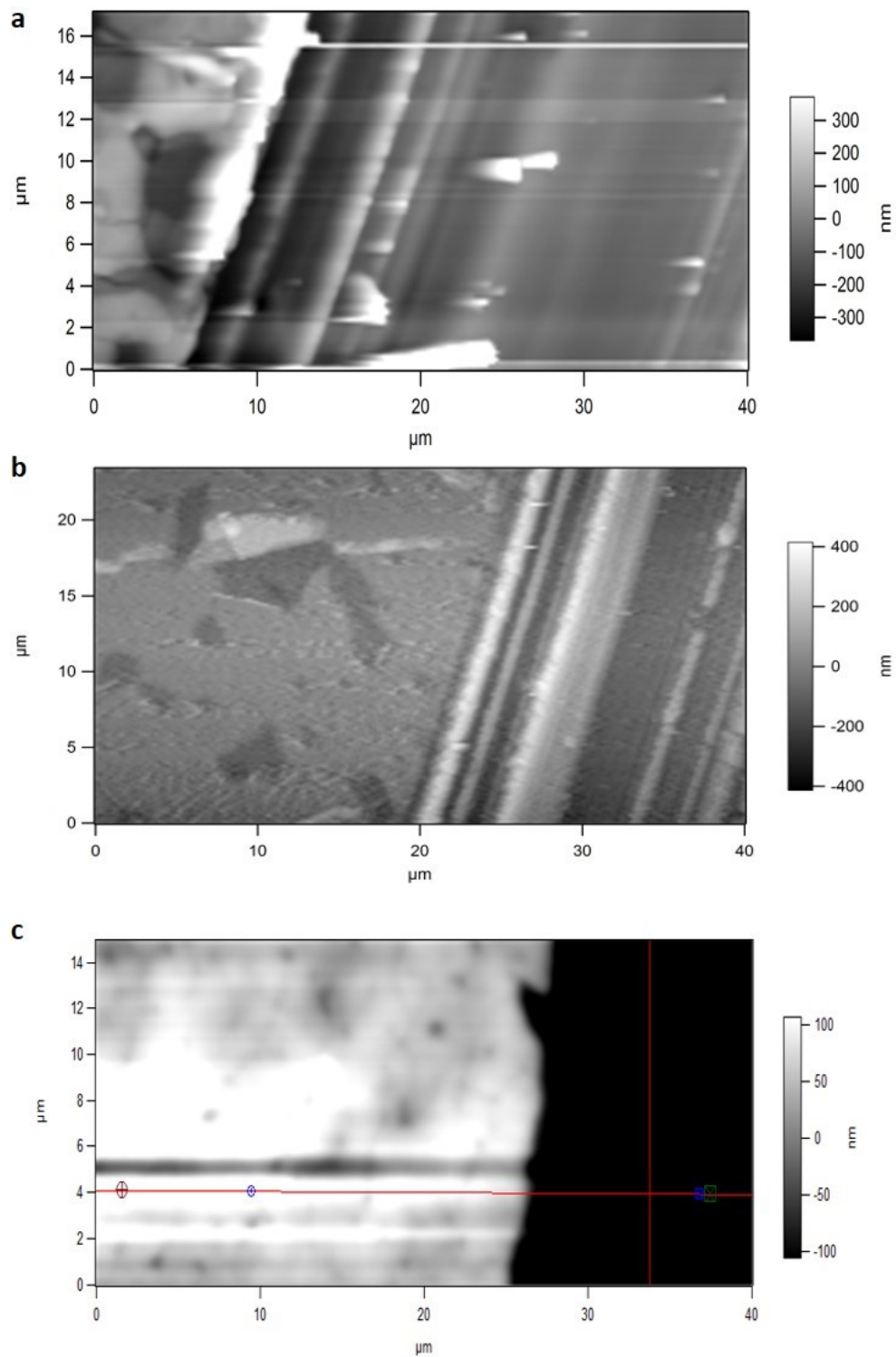


Figure S12. AFM images of three layer (a) 3.2 nm PbSe NC SL, (b) 4.5 nm PbSe NC SL, and (c) BNSL self-assembled with both 3.2 nm and 4.5 nm PbSe NC capped with oleic acid. The average monolayer film thickness is (a) 112 nm, (b) 76 nm and (c) 120 nm.

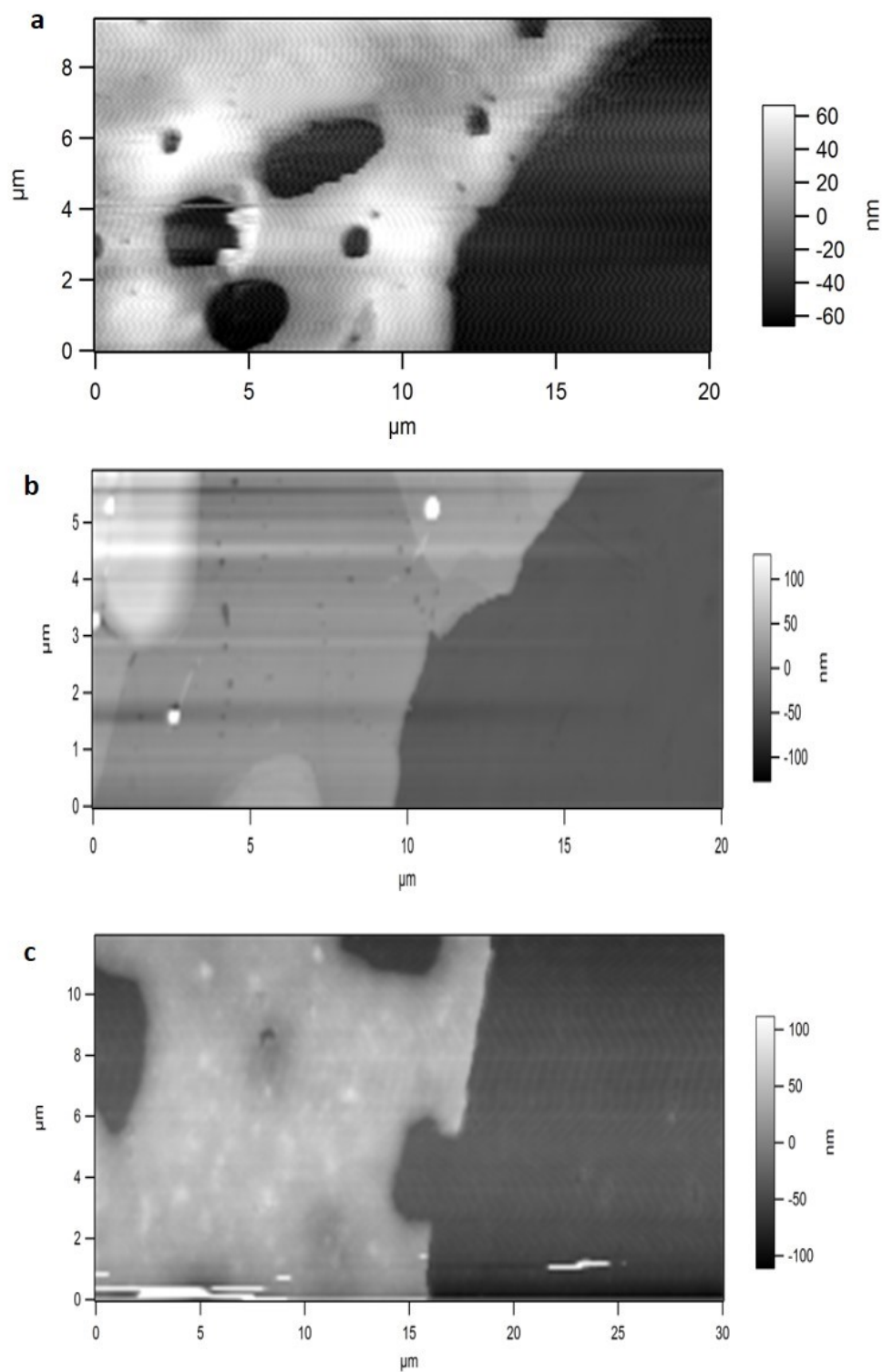


Figure S13. AFM images of three layer (a) 3.2 nm PbSe NC SL 3-MPA, (b) 4.5 nm PbSe NC SL MPA, and (c) BNSL self-assembled with both 3.2 nm and 4.5 nm PbSe NC MPA. The average monolayer film thickness is (a) 82.2 nm, (b) 64.9 nm and (c) 85.8 nm.

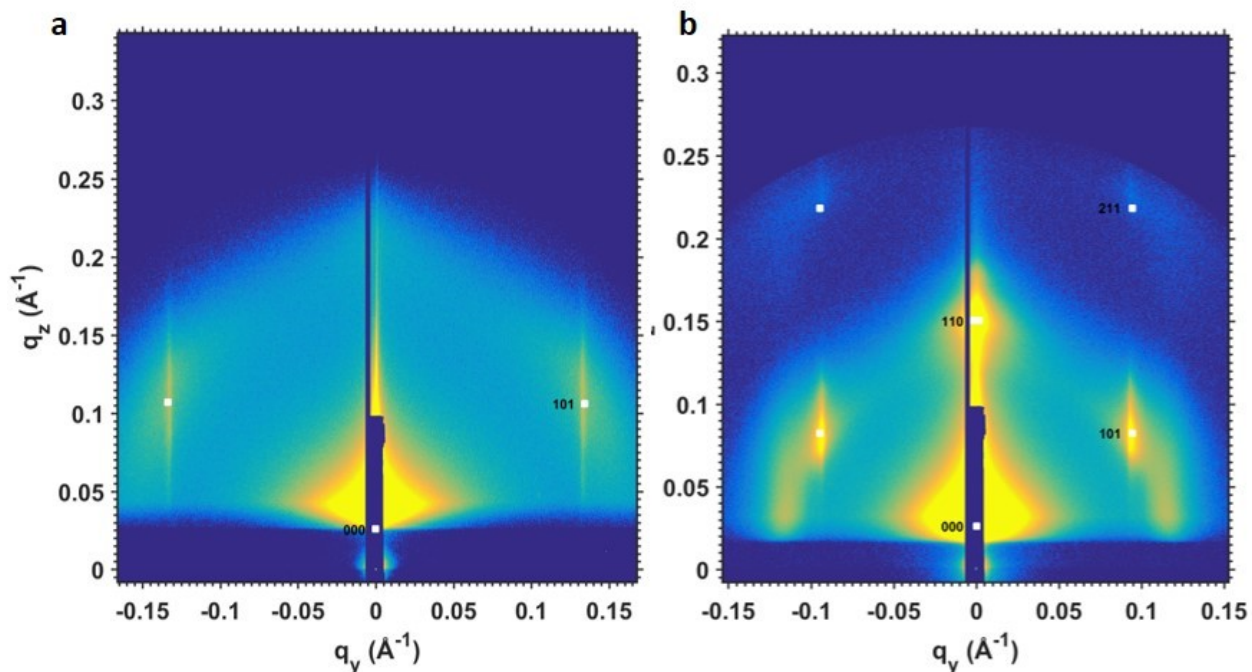


Figure S14. GISAXS patterns and simulation of (a) 3.2 nm and (b) 4.5 nm PbSe NC SL, ligand exchanged with MPA. The lattice constants are listed in Table S3.

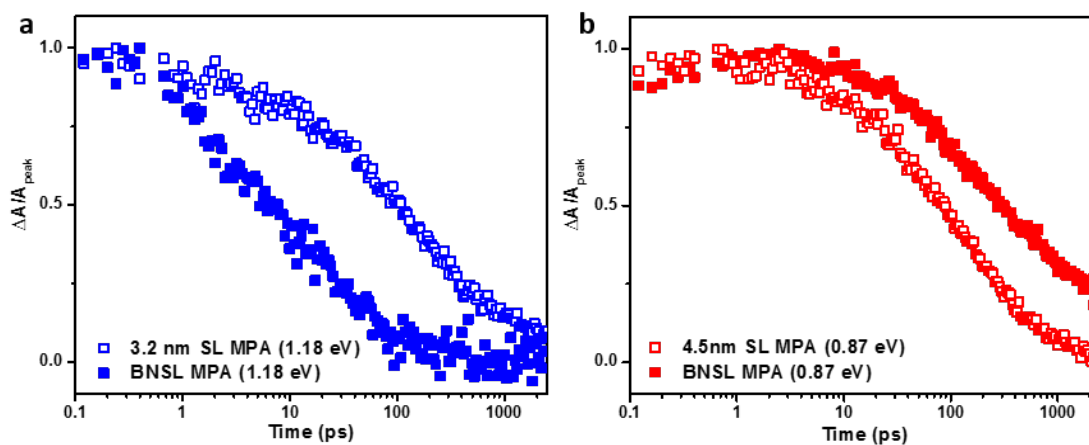


Figure S15. (a) 1S bleach dynamics of 3.2 nm PbSe NC in single component, BNSL over 2.5 ns, probed at 1.18 eV. (b) 1S bleach dynamics of 4.5 nm PbSe NC in single component and binary superlattice over 2.5 ns, probed at 0.87 eV. NCs all capped with MPA.